



OPEN

## Structural elastic and thermodynamic properties of cubic CsCl type MgCa using ab initio approach

Abdelfateh Benmakhlof<sup>1</sup>, Nadhira Bioud<sup>2,3</sup>, M. A. Ghebouli<sup>4,5</sup>, M. Fatmi<sup>4</sup>✉, Razan A. Alshgari<sup>6</sup>, Saikh Mohammad<sup>6</sup> & Mika Sillanpää<sup>7,8</sup>

The CsCl-structured MgCa intermetallic compound was examined through computational quantum mechanics, employing DFT methodology via CASTEP implementation. Analysis of volumetric energy correlations revealed fundamental parameters: a 3.868 Å lattice dimension, 27.99 GPa compressibility factor, and corresponding pressure coefficient of 3.70. The LDA framework produced crystallographic and mechanical flexibility values consistent with previously published computational findings. Thermophysical behavior was quantified using Debye quasi-harmonic approximations spanning thermal conditions (0–800 K) and compression states (0–10 GPa). Under standard reference conditions ( $P=0$  GPa,  $T=0$  K), the characteristic vibrational temperature parameter reached 319.23 K, exhibiting remarkable concordance with the independently calculated elastic-based estimate of 321.1 K.

**Keywords** MgCa intermetallic compound, DFT, Ab-initio calculations, Elastic constants, Structural and thermodynamic properties.

Magnesium-based binary alloys are highly promising materials for various applications, including microstructure engineering, the automotive sector, and aerospace industries<sup>1</sup>. Magnesium (Mg) is well known for being an exceptionally lightweight metal, with a density and mechanical properties comparable to natural bone. This characteristic makes it advantageous for biomedical applications, particularly in promoting new bone tissue growth while reducing stress shielding effects commonly associated with conventional metallic implants<sup>2</sup>. The Mg–Ca system has been studied theoretically by Zhou and Gong<sup>2</sup> using first-principles calculations based on density functional theory (DFT) within the generalized gradient approximation (GGA). Their findings indicate that the MgCa compound undergoes a structural transformation from the body-centered cubic (BCC) phase to the hexagonal close-packed (HCP) phase at a pressure of 10.66 GPa. Groh<sup>3</sup> developed interatomic potentials for both pure calcium (Ca) and the Mg–Ca binary system and employed the second nearest-neighbor modified embedded-atom method (MEAM) to calculate their elastic constants, thermal properties, and other physical parameters across different phases. Daoud et al.<sup>4</sup> utilized the pseudopotential plane-wave (PP-PW) approach within the DFT framework to study the impact of high pressure (up to 16 GPa) on the structural parameters and elastic properties of the MgCa intermetallic compound in the cubic CsCl-type (B2) structure. Their results revealed a significant deviation from the Cauchy condition, indicating the presence of strong non-central many-body interactions in the (B2) MgCa compound. Additionally, Rekab-Djabri et al.<sup>5</sup> investigated the ground-state parameters, elastic properties, and electronic structure of the Mg<sub>3</sub>Ca intermetallic compound. They examined its structural behavior in various phases, including Cu<sub>3</sub>Au (L1<sub>2</sub>), AlFe<sub>3</sub> (D0<sub>3</sub>), αReO<sub>3</sub> (B09), and CuTi<sub>3</sub> (L60) structures. Their findings showed that under compression, Mg<sub>3</sub>Ca transitions from the D0<sub>3</sub> to the D0<sub>9</sub> phase at

<sup>1</sup>Laboratory of Materials and Electronic Systems Faculty of Sciences and Technology, Mohamed El Bachir El Ibrahimi University of Bordj BouArreridj, Bordj BouArreridj 34000, Algeria. <sup>2</sup>Faculty of Sciences and Technology, University of Mohamed El Bachir El Ibrahimi-Bordj BouArreridj, Bordj BouArreridj 34000, Algeria. <sup>3</sup>Laboratory of Optoelectronic and Compounds, Faculty of Sciences, Ferhat Abbas University of Setif 1, Setif 19000, Algeria. <sup>4</sup>Research Unit on Emerging Materials (RUEM), University Ferhat Abbas of Setif 1, Setif 19000, Algeria. <sup>5</sup>Department of Chemistry, Faculty of Science, University of M'sila University, Pole, Road BourdjBouArreiridj, M'sila 28000, Algeria. <sup>6</sup>Department of Chemistry, College of Science, King Saud University, Riyadh 11451, Saudi Arabia. <sup>7</sup>Department of Biological and Chemical Engineering, Aarhus University, Norrebrogade 44, Aarhus 8000, Aarhus C, Denmark. <sup>8</sup>Centre of Research Impact and Outcome, Chitkara University, Institute of Engineering and Technology, Chitkara University, Rajpura 140401, Punjab, India. ✉email: Fatmimessaoud@yahoo.fr

a pressure of 29.96 GPa using LDA and at 25.1 GPa using GGA. This study aims to investigate the structural, mechanical, and thermodynamic properties of the studied compound using ab initio calculations based on DFT. The analysis of its mechanical and thermal stability helps assess its potential for various technological applications of the MgCa intermetallic compound in the cubic CsCl-type structure. The obtained results offer promising prospects for integrating this material into devices requiring high structural and thermal resistance. Moreover, they provide a valuable reference for future experimental research. This work can thus contribute to the optimization of materials used in electronics, protective coatings, and high-performance alloys.

## Calculation method

Our computational framework utilized DFT methodology via the CASTEP implementation<sup>6</sup>, employing plane-wave pseudopotential techniques. Exchange-correlation effects were addressed through CA-PZ functional LDA approximations<sup>7,8</sup>, while ultrasoft pseudopotentials characterized electron-ion interactions<sup>9</sup>. The numerical parameters included a 450 eV energy cutoff for plane-wave expansion and Brillouin zone sampling across a  $16 \times 16 \times 16$  Monkhorst-Pack grid<sup>10</sup>. Convergence thresholds encompassed  $5 \times 10^{-6}$  eV/atom for energy differential, alongside specified geometric constraints (0.02 GPa,  $5 \times 10^{-4}$  Å, and 0.01 eV/Å for forces). Thermophysical behavior was investigated utilizing quasi-harmonic Debye approximations<sup>11</sup> across compression states (0–10 GPa) and thermal conditions (0–800 K). Given the absence of experimental measurements for CsCl-structured MgCa, this investigation provides computational predictions of fundamental physical properties through quantum mechanical calculations.

## Results and discussion

### Equilibrium structural

The intermetallic MgCa compound exhibits cubic crystallization with the CsCl structural arrangement. This configuration features equivalent dimensional parameters along all axes ( $a=b=c$ ) and right-angled intersections ( $\alpha=\beta=\gamma=90^\circ$ ). Each fundamental crystallographic unit incorporates a single magnesium atom and one calcium atom. Researchers typically derive equilibrium structural characteristics by analyzing the correlation between volumetric variations and total energy states<sup>12,13</sup>.

From Fig. 1, which depicts the total energy  $E_{\text{Tot}}$  as a function of volume  $V$ , the static structural parameters can be determined. Specifically, the lattice constant ( $a_0$ ) is obtained from the volume corresponding to the minimum total energy ( $E_0$ ). Additionally, the ( $B_0$ ) and  $B_0'$  are extracted by fitting by (BM-EOS) equation, which is given by<sup>14,15</sup>:

$$E(V) - E_0 = \frac{9V_0B_0}{16} \left\{ B_0' \left[ \left( \frac{V_0}{V} \right)^{2/3} - 1 \right]^3 + \left[ \left( \frac{V_0}{V} \right)^{2/3} - 1 \right]^2 \left[ 6 - 4 \left( \frac{V_0}{V} \right)^{2/3} \right] \right\} \quad (1)$$

The Birch-Murnaghan equation of state incorporates both  $B_0$  (the bulk modulus) and its pressure derivative  $B_0'$  as fundamental parameters characterizing the material's response to compression. The pressure derivative of the bulk modulus at zero pressure, mathematically defined as:  $B_0' = \frac{\partial B}{\partial P}$  at  $P=0$ . This parameter describes how the bulk modulus changes with pressure at the equilibrium state.

The obtained values of  $a_0$ ,  $B_0$ , and  $B_0'$  as well as the minimum total energy  $E_0$  for MgCa intermetallic compound are summarized in Table 1.

These parameters have also been analyzed and compared with other theoretical results, showing strong agreement. For instance, the difference between our lattice constant (3.868 Å) and the theoretical value (3.96 Å) is less than 2.4%<sup>2</sup>. Similarly, our bulk modulus value (27.99 GPa) deviates by approximately 9.75% from the theoretical value (25.26 GPa). Additionally, our calculated pressure derivative of the bulk modulus ( $B_0'=3.70$ ) is slightly lower than the theoretical value (4.05) reported by Daoud *et al.*<sup>4</sup>. It is worth noting that the LDA approach generally predicts lower equilibrium lattice constants than the GGA method.

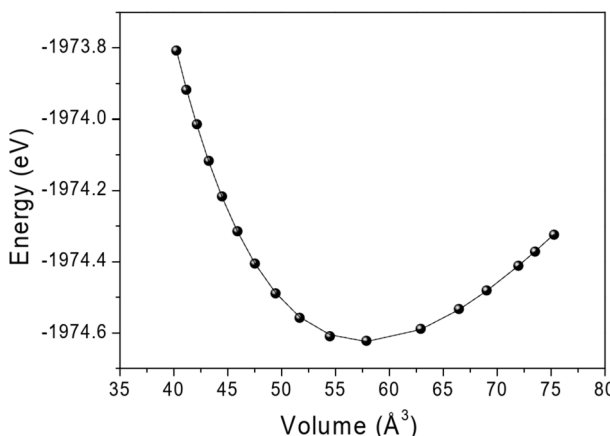


**Fig. 1.** Plot of the total energy versus the volume of primitive unit cell for CsCl-type structure MgCa.

Parameter	$a_0$ (Å)	$B_0$ (GPa)	$B'_0$	$E_0$ (eV)
This work (DFT-LDA)	3.868	27.99	3.70	-1974.62
Ref. [2] DFT-GGA	3.96	25.26	-	-
Ref. [3] MEAM	3.96	25.16	-	-
Ref. [4] DFT-GGA	3.9764	23.33	4.05	-

**Table 1.** Equilibrium structural parameters  $a_0$ (Å), bulk modulus  $B_0$ (GPa), its pressure derivative  $B'_0$  and total energy  $E_0$ (eV) for (B2) MgCa, in comparison with the theoretical data existing in the literature<sup>2-4</sup>.

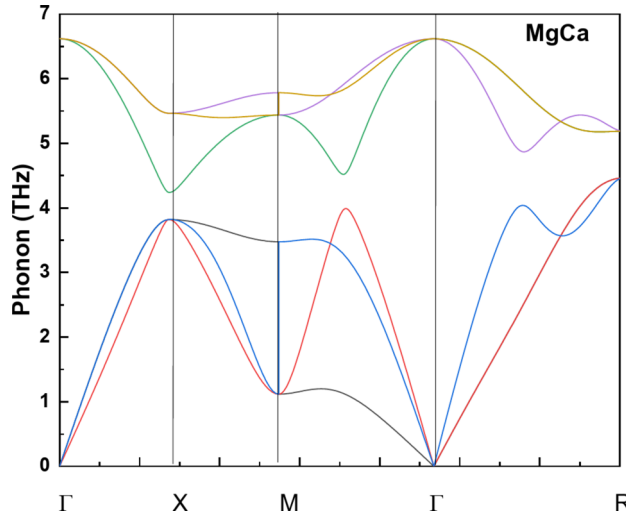


**Fig. 2.** Phonon dispersion curve of the MgCa compound along the Brillouin zone for (B2) MgCa.

Parameter	$C_{11}$ (GPa)	$C_{12}$ (GPa)	$C_{44}$ (GPa)	$B$ (GPa)
This work (DFT-LDA)	38.25	23.80	28.07	28.62
Ref. [2] DFT-GGA	32.28	21.75	24.94	25.26
Ref. [3] MEAM	39.74	18.59	21.61	25.64
Ref. [4] DFT-GGA	37.60	19.82	25.73	25.75

**Table 2.** Elastic constants  $C_{ij}$ (GPa) and aggregate bulk modulus  $B$ (GPa) for MgCa.

Moreover, the melting point  $T_m$  is correlated with other physical parameters, particularly the bulk modulus  $B$ , for cubic-structured solids. It follows the empirical relation  $B: T_m$  (K) =  $9.3 \times B$  (K/GPa) + 607 (K)<sup>16</sup>. By substituting our bulk modulus value ( $B_0 = 27.99$  GPa) into this equation, we estimate the melting point of the MgCa intermetallic compound to be 867.3 K. This figure is little more than the  $775 \pm 300$  K theoretical prediction. To our knowledge, no experimental data on the melting point of MgCa intermetallic compounds is available in the literature. Figure 2 illustrates the phonon dispersion curve of the MgCa compound along the Brillouin zone.

The absence of imaginary frequencies confirms the dynamical stability of the cubic CsCl-type phase, which allows for the investigation of the elastic and thermodynamic properties of the compound, especially in the absence of experimental results for this structure.

### Elastic properties

The elastic constants are essential for understanding the mechanical properties of materials<sup>17</sup>. For cubic crystals, the bulk modulus  $B$  may be obtained from the elastic constants  $C_{ij}$  as follows:  $B = (2C_{12} + C_{11})/3$ . Our calculated values of the elastic constants  $C_{ij}$  and the bulk modulus for (B2) MgCa are summarized in Table 2. The value 28.62 GPa of the bulk modulus  $B$  obtained from the elastic constants is in excellent agreement with the value 27.99 GPa obtained from the fit of the (E-V) data by the BM-EO (Eq. 1). The discrepancy on the bulk modulus  $B$  between these two values is only 2.2%. Furthermore, our values of the elastic constants  $C_{ij}$  as well as that of the bulk modulus  $B$  are in reasonable agreement in comparison with other data existing in the literature. Note that the LDA approach gives higher values for the elastic constants  $C_{ij}$  and the bulk modulus than the GGA ones.

The thermodynamic properties of MgCa were investigated using the quasi-harmonic Debye model, which allows us to determine the temperature and pressure dependencies of key physical parameters. This model is based on the  $G(T, P)$ , which is related to the Helmholtz free energy  $F(T, V)$  as follows:

$$PV + F(T, V) = G(T, P) \quad (2)$$

where  $F(T, V)$  is expressed as:

$$F_{vib}(T, V) + E_{tot}(V) = F(T, V) \quad (3)$$

Here,  $E_{tot}(V)$  is the total energy obtained from DFT calculations, while the vibrational contribution to the free energy,  $F_{vib}(T, V)$  is calculated using the Debye approximation:

$$F_{vib}(T, V) = 9k_B T \left[ \frac{\theta_D}{8T} + \ln \left( 1 - e^{-\frac{\theta_D}{T}} \right) - D \frac{\theta_D}{T} \right] \quad (4)$$

The Debye temperature  $\theta_D$  is a key fundamental parameter in solid-state physics, which is closely associated with various physical properties, including melting temperature, specific heat and elastic constants<sup>17,18</sup>. At above  $\theta_D$ , the thermal vibrations become more important than the quantum effects conducting that the crystal behaves classically<sup>19,20</sup>. At low temperatures, vibrational excitations are primarily due to acoustic modes. The Debye temperature calculated from elastic constants at low temperatures is identical to that determined from specific heat measurements. The Debye temperature  $\theta_D$  was deduced from the speed of the sound  $v_m$  as follows:

$$\theta_D = \frac{h}{k_B} \left( \frac{3}{4\pi V_a} \right)^{1/3} \nu_m \quad (5)$$

where  $h$  is the Plank's constant,  $V_a$  is the atomic volume and  $k_B$  is the Boltzmann's constant. The average sound velocity  $v_m$  is given by<sup>21,22</sup>:

$$v_m = \left[ \frac{1}{3} \left( \frac{2}{v_l^3} + \frac{1}{v_t^3} \right) \right]^{-1/3} \quad (6)$$

where  $v_l$  and  $v_t$  are the longitudinal and transverse sound velocity, respectively. They are calculated from the following equations:

$$v_l = \left( \frac{3B + 4G}{3\rho} \right)^{1/2} \text{ and } v_t = \left( \frac{G}{\rho} \right)^{1/2} \quad (7)$$

Using the values of the elastic constants  $C_{ij}$  obtained in this study for the studied material, the computation yielded average value of the shear modulus  $G = 16.38$  GPa. The average shear modulus ( $G$ ) was calculated using the Voigt-Reuss-Hill (VRH) homogenization scheme, which is the arithmetic mean of the Voigt and Reuss bounds. For cubic crystals, the Voigt bound ( $G_V$ ) and Reuss bound ( $G_R$ ) are calculated through the following relations:

$$G_V = (C_{11} - C_{12} + 3C_{44})/5 \quad (8)$$

$$G_R = \frac{5(C_{11} - C_{12}) \times C_{44}}{4 \times C_{44} + 3(C_{11} - C_{12})} \quad (9)$$

Therefore, the average shear modulus according to the VRH scheme is:

$$G = \frac{G_V + G_R}{2} \quad (10)$$

The calculated of the  $\rho$ ,  $v_p$ ,  $v_t$ ,  $v_m$  and  $\theta_D$  for CsCl-type structure MgCa intermetallic compound are given in Table 3.

All the elastic constants  $C_{ij}$  obtained in this work are slightly higher than the theoretical ones reported by Daoud et al.<sup>4</sup>, one can notice that the calculated values of the sound velocities ( $v_p$ ,  $v_t$  and  $v_m$ ) and the Debye temperature  $\theta_D$  for MgCa are slightly lower than their theoretical ones. The percentage deviation is around 5.16% for  $v_m$ ; while the discrepancy on  $\theta_D$  is only around 2.35%. Note that the LDA approach gives higher values for  $v_p$ ,  $v_t$ ,  $v_m$ ,  $\rho$  and  $\theta_D$  than the GGA ones in the case  $M_2XC$  ( $M = Cr$  and  $Ti$ ,  $X = Al$  and  $Ga$ ) ternary compounds<sup>17</sup>.

### Thermodynamic properties

The thermodynamic properties are essential parameters for studying chemical reactivity and crystal stability<sup>23,24</sup>. Pressure is a fundamental thermodynamic variable that can be used to transfer matter from one state to another.

Parameter	$\rho$ (g/cm <sup>3</sup> )	$v_l$ (km/s)	$v_t$ (km/s)	$v_m$ (km/s)	$\theta_D$ (K)
This work (DFT-LDA)	1.844	5.231	2.980	3.313	321.1
Ref. [4]DFT-GGA	1.700	5.323	3.145	3.484	328.65

**Table 3.** Mass density, longitudinal  $v_p$ , transversal  $v_t$  and average  $v_m$  sound velocities and Debye temperature  $\theta_D$  for MgCa.

The effect of pressure (0, 2, 4, 6, 8 and 10 GPa) and temperature on the unit cell volume for MgCa is presented in Fig. 3(a, b). Notice that the unit cell volume decreases with compression at (0, 300, 600 and 800 K). The bond length is decreasing, which causes the volume to shrink under the compression action. In other hand, the elevation of temperature conducts to an expansion of the bond-length. Similar behavior has been observed for different materials such as for cubic zinc-blende AlP, for copper scandium (CuSc) intermetallic compound and for (B3) boron nitride (*c*-BN) compound<sup>25</sup> at temperatures 300, 600 and 900 K and in the pressure range 0 to 36 GPa.

At temperatures of 0, 300, 600 and 800 K, the fits of the unit cell volume  $V$  values for MgCa intermetallic compound obey the following quadratic expressions, respectively:

$$V = 58.29 - 1.78p + 6.20 \times 10^{-2}p^2 \quad (11)$$

$$V = 59.52 - 1.97p + 7.20 \times 10^{-2}p^2 \quad (12)$$

$$V = 61.63 - 2.30p + 8.96 \times 10^{-2}p^2 \quad (13)$$

$$V = 63.35 - 2.58p + 10.06 \times 10^{-1}p^2 \quad (14)$$

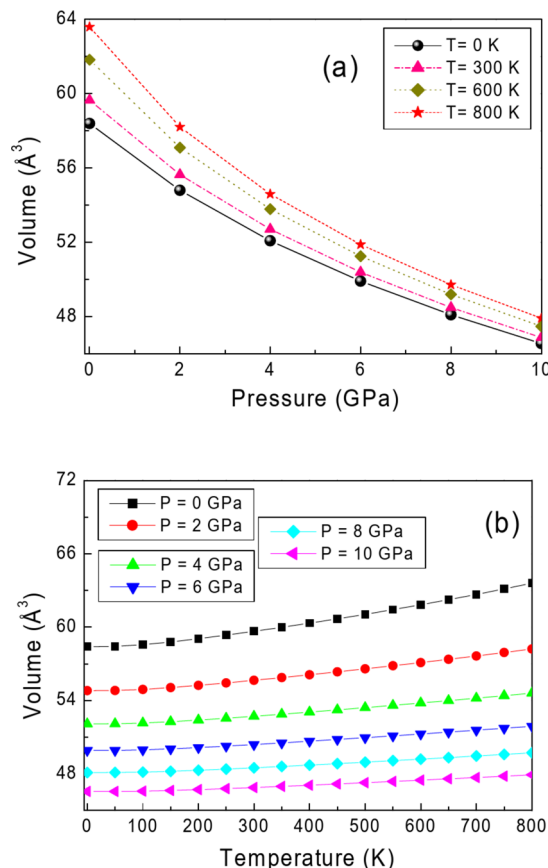
where the unit cell volume  $V$  is expressed in  $\text{\AA}^3$  and the pressure is expressed in GPa.

According to the laws of thermodynamics, the isothermal bulk modulus  $B_T$  may be obtained from the following formula<sup>11</sup>:

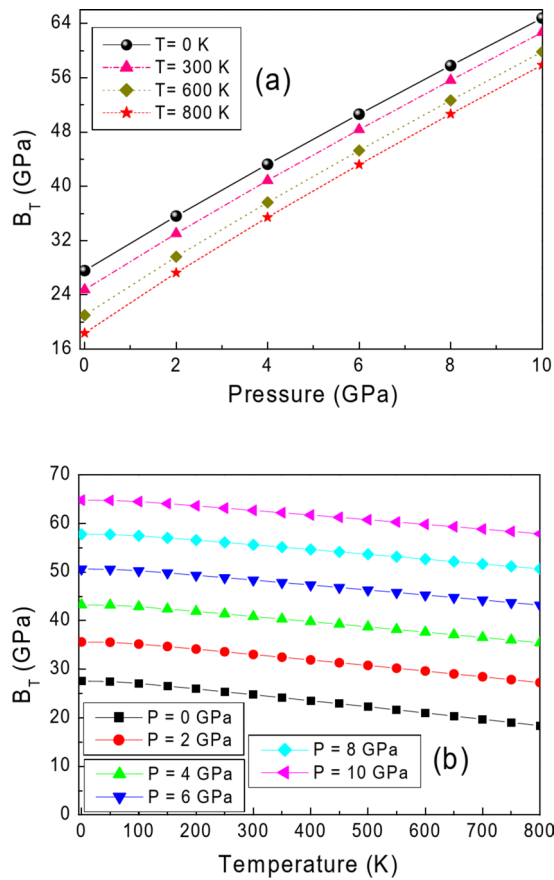
$$B_T = -V \left( \frac{\partial p}{\partial V} \right)_T \quad (15)$$

Figure 4 shows the isothermal bulk modulus  $B_T$  for CsCl-type structure MgCa versus pressure and temperature. It increases with increasing pressure and decreases with increasing temperature. Similar behavior has been observed for AlP semiconducting compound, for copper scandium (CuSc) intermetallic compound at temperatures 0, 300, 600 and 1000 K and pressure ranging from 0 to 12 GPa, for *c*-BN binary compound, for  $\text{Co}_2\text{MnAl}$ ,  $\text{Co}_2\text{MnGe}$  and  $\text{Co}_2\text{MnSn}$  ternary compounds<sup>26</sup> and for the ordered  $\text{Ge}_{0.5}\text{Sn}_{0.5}$  in cubic zinc-blende phase<sup>27</sup>.

The pressure derivative of the isothermal bulk modulus  $B'_T$  is given by the following formula<sup>11</sup>:



**Fig. 3.** Effect of pressure and temperature on unit cell volume for CsCl-type structure MgCa intermetallic compound.



**Fig. 4.** Isothermal bulk modulus  $B_T$  for CsCl-type structure MgCa versus pressure and temperature.

$$B'_T = (\partial B_T / \partial p)_T \quad (16)$$

The variation of  $B'_T(p, T)$  as a function of compression at different temperatures (0, 300, 600 and 800 K) and versus temperature at different pressures (0, 2, 4, 6, 8 and 10 GPa) for MgCa are displayed in Fig. 5(a, b). We observe that  $B'_T(p, T)$  decreases as pressure enhances and increases with the augmentation of 0 to 800 K. At  $p=10$  GPa,  $B'_T(p, T)$  changes slowly with arising of the temperature. The value 4.15 of  $B'_T(p, T)$  obtained at  $p=0$  and  $T=0$  K is slightly higher than that 3.70 of  $B'_0$  obtained from the fit with Eq. (1).

The following quadratic expressions are the different fits on  $B'_T$  as a function of temperature (in K) at 0, 2, 4, 6, 8 and 10 GPa, respectively:

$$B'_T = 4.15 + 4.21 \times 10^{-4}T + 3.36 \times 10^{-7}T^2 \quad (17)$$

$$B'_T = 3.90 + 30.06 \times 10^{-4}T + 1.30 \times 10^{-7}T^2 \quad (18)$$

$$B'_T = 3.74 + 2.29 \times 10^{-4}T + 0.69 \times 10^{-7}T^2 \quad (19)$$

$$B'_T = 3.63 + 1.75 \times 10^{-4}T + 0.42 \times 10^{-7}T^2 \quad (20)$$

$$B'_T = 3.54 + 1.33 \times 10^{-4}T + 0.28 \times 10^{-7}T^2 \quad (21)$$

$$B'_T = 3.47 + 0.99 \times 10^{-4}T + 0.20 \times 10^{-7}T^2 \quad (22)$$

In the quasi-harmonic model, the Debye temperature  $\theta_D$  may be calculated employing the following expression<sup>11</sup>:

$$\theta_D = \frac{\hbar}{k} (6\pi^2 V^{0.5} n)^{1/3} f(\sigma) (B_s/M)^{1/2} \quad (23)$$

where  $\hbar$  is the reduced Planck constant,  $M$  is the molecular mass per primitive cell,  $B_s$  is the adiabatic bulk modulus,  $k$  is the Boltzmann constant,  $f(\sigma)$  is functional of other quantity  $\sigma$  which is the Poisson ratio.

The variation of  $\theta_D$  as a function of compression at (0, 300, 600 and 800 K) and versus temperature at (0, 2, 4, 6, 8 and 10 GPa) for MgCa are displayed in Fig. 6(a, b).

As pressure rises, the Debye temperature rises monotonically; conversely, as temperature rises, it falls. At a fixed low value of pressures (0, 2, 4 and 6 GPa), the  $\theta_D$  decreases with rising temperature for MgCa, while for high

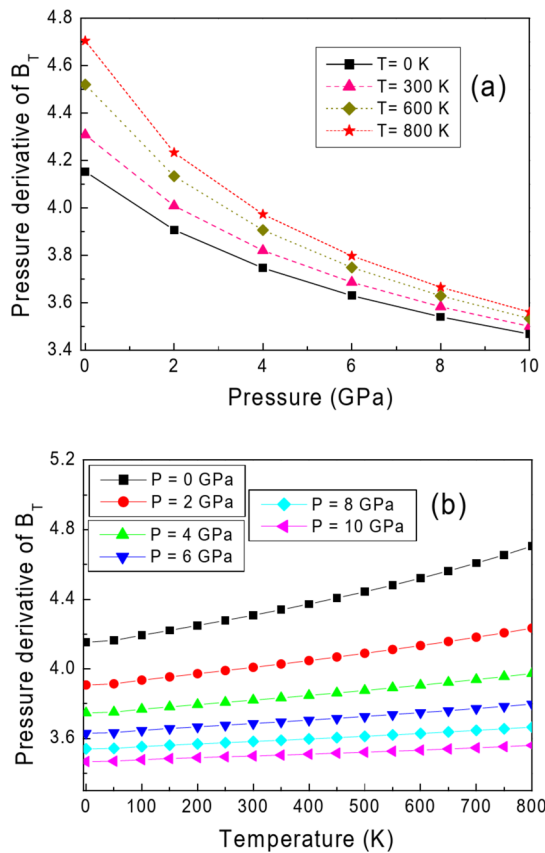


**Fig. 5.** Effect of pressure and temperature on  $B_T'$  for MgCa material.

values of pressure (8 and 10 GPa) the  $\theta_D$  for MgCa becomes unchanged with rising temperature. An increase in the Debye temperature  $\theta_D$  with pressure has also been observed for calcium oxide (CaO) compound<sup>28</sup>, for cubic rock-salt cadmium oxide (CdO) semiconducting compound<sup>29</sup>, for cubic zinc-blende gallium antimonide (GaSb) compound<sup>30</sup>, for cubic zinc-blende boron antimonide (BSb) semiconducting compound<sup>31</sup>, for cubic perovskite  $\text{CsCdF}_3$  ternary material<sup>32</sup> and for beta silicon carbide (3 C-SiC)<sup>33</sup>. At  $p=0$  and  $T=0$  K, our calculation yielded value of the Debye temperature  $\theta_D \sim 319.23$  K, which is in excellent agreement with our value 321.1 K obtained from the elastic constants. The discrepancy on  $\theta_D$  between the two values obtained from the quasi-harmonic Debye model and the elastic constants is less than 0.60%. The following quadratic expressions are the different fits on  $\theta_D$  as a function of pressure (in GPa) at 0, 300, 600 and 800 K, respectively:

$$\theta_D = 319.97 + 20.14p - 4.92 \times 10^{-1} p^2 \quad (24)$$

$$\theta_D = 307.13 + 21.63p - 5.64 \times 10^{-1} p^2 \quad (25)$$

$$\theta_D = 2860.05 + 23.96p - 6.83 \times 10^{-1} p^2 \quad (26)$$

$$\theta_D = 269.86 + 25.96p - 7.92 \times 10^{-1} p^2 \quad (27)$$

where the volume  $V$  is expressed in  $\text{\AA}^3$  and the pressure is in GPa.

The structural behaviour under temperature effect of material may be explicated by the thermal expansion coefficient<sup>34</sup>. The volumetric thermal expansion coefficient  $\alpha$  was given by the following formula:

$$\alpha = -\frac{1}{V} \left( \frac{\partial V}{\partial T} \right)_p \quad (28)$$

where  $V$  is the volume,  $T$  is the temperature and  $p$  is the pressure.

The effect of pressure (0, 2, 4, 6, 8 and 10 GPa) and temperature on the volumetric thermal expansion coefficient for MgCa is presented in Fig. 7 (a, b), respectively.

We observe that the volumetric thermal expansion coefficient  $\alpha$  of MgCa decreases with compression and enhances with temperature from 0 to 800 K. The increasing of  $\alpha$  with increasing temperature and the decreasing of  $\alpha$  with increasing pressure was observed also for the alkali metal chalcogenide  $\text{K}_2\text{S}$  binary compound, for the perovskite oxide  $\text{SnTiO}_3$  in the cubic phase<sup>34</sup>, for (B2) MgCu material<sup>35</sup> and for the superconductor  $\text{Nb}_3\text{Ga}$  intermetallic binary compound<sup>36</sup> at pressures 0, 10, 20, 30 and 40 GPa, and temperature ranging from 0 to

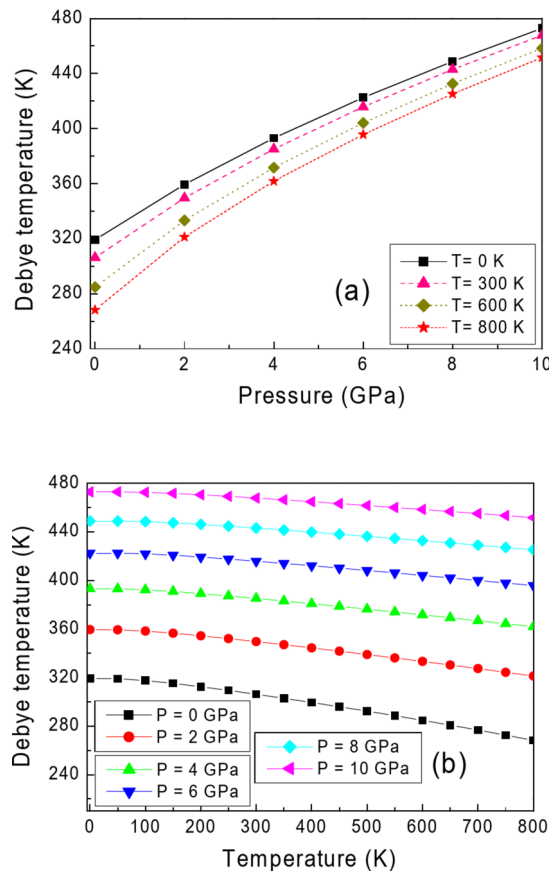


**Fig. 6.** Impact of pressure at 0, 300, 600 and 800 K and temperature at 0, 2, 4, 6, 8 and 10 GPa on Debye temperature for CsCl-type structure MgCa.

1000 K. At high pressures (8 and 10 GPa) and high temperatures ( $T > 500$  K), the volumetric thermal expansion coefficient changes slowly with arising of the temperature. At ambient pressure the thermal expansion coefficient can be represented simply as<sup>37</sup>:

$$a(T) = a + bT - c/T^2 \quad (29)$$

For MgCa, the numerical values of the constants  $a$ ,  $b$  and  $c$  are found  $7.68 \times 10^{-5}/\text{K}$ ,  $9.35 \times 10^{-8}/\text{K}^2$  and  $1.5 \times 10^{-1}$  K, respectively.

The constant pressure heat capacity  $C_p$  was given by the following formula<sup>11</sup>:

$$C_p = \left( \frac{\partial H}{\partial T} \right)_p \quad (19)$$

where  $H$  is the enthalpy.

The variation of the constant pressure heat capacity  $C_p$  as a function of pressure at 100, 300, 600 and 800 K for MgCa was illustrated in Fig. 8 (a), while the variation of  $C_p$  as a function of temperature  $T$  at (0, 2, 4, 6, 8 and 10 GPa) was shown in Fig. 8 (b).

We observe that the constant pressure heat capacity  $C_p$  of MgCa decreases with compression and increases with temperature from 0 to 800 K. The increasing of  $C_p$  with increasing of temperature and decreasing of  $C_p$  with increasing pressure was observed also for aluminum phosphide (AlP) binary semiconductor<sup>12</sup>, for the alkali metalchalcogenide  $\text{K}_2\text{S}$  binary compound<sup>20</sup> and for CsCl-type structure MgCu binary intermetallic compound<sup>35</sup>.

Except the data reported on the entropy and specific heat capacity  $C_V$  by Daoud et al.<sup>4</sup>, we think that there is no data or results reported in the literature on the thermodynamic properties for MgCa with CsCl-type structure.

## Conclusion

In this study, we investigated the structural parameters and elastic constants of CsCl-type structure MgCa intermetallic compound. We use the plane-wave pseudopotential approach within the DFT. Our calculated

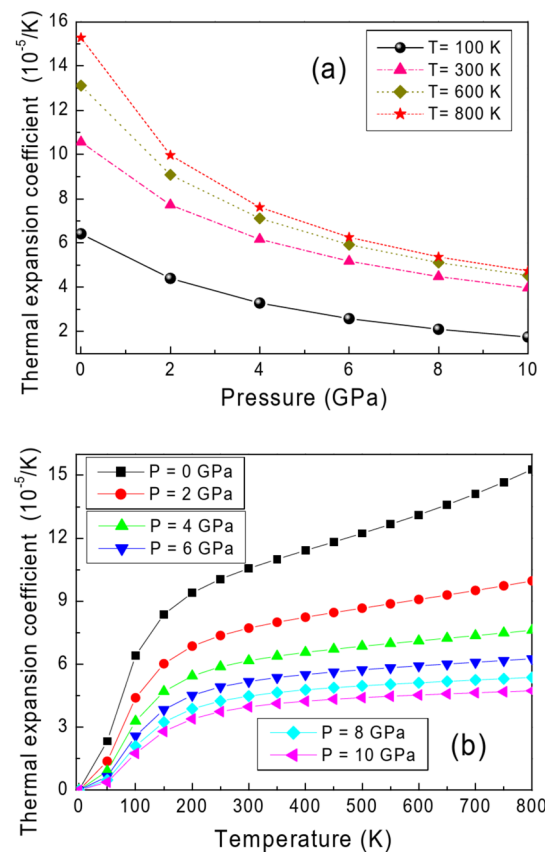


**Fig. 7.** Impact of pressure at 100, 300, 600 and 800 K and temperature at 0, 2, 4, 6, 8 and 10 GPa on volumetric thermal expansion coefficient for MgCa.

structural parameters and mechanical properties agreed well with other data reported in the literature. The melting temperature  $T_m$  of CsCl-type structure MgCa has been also evaluated. Furthermore, the impact of pressure varied within 0–10 GPa and temperature varied within 0–800 K on the thermodynamic properties of MgCa have been determined using the quasi-harmonic Debye model. At  $p=0$  and  $T=0$  K, our calculation yielded value of the Debye temperature  $\sim 319.23$  K, which concords very well with the value 321.1 K obtained from the elastic constants, while at  $p=0$  and  $T=800$  K, the Debye temperature of CsCl-type structure MgCa reaches the value  $\sim 268.21$  K.

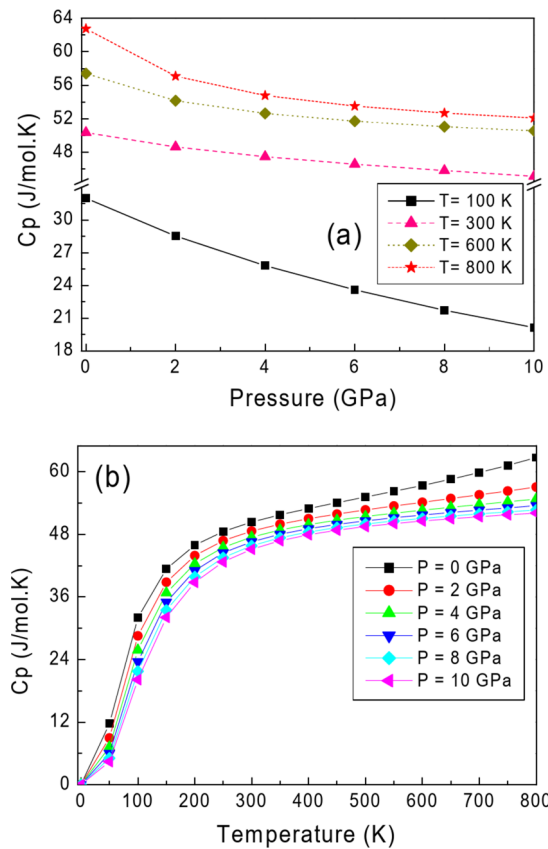


**Fig. 8.** Plot between heat capacity  $C_p$  and pressure at various temperatures and between  $C_p$  and temperature at various pressures for MgCa.

## Data availability

Data underlying the results presented in this paper are not publicly available at this time but may be obtained from the author (fatemimessaoud@yahoo.fr) upon reasonable request.

Received: 11 December 2024; Accepted: 21 May 2025

Published online: 29 May 2025

## References

1. Rameshkumar, S., Jaiganesh, G. & Jayalakshmi, V. Structural, phonon, elastic, thermodynamic and electronic properties of Mg-X (X= La, Nd, Sm) intermetallics: the first principles study. *J. Magnes. Alloys.* **7**, 166–185. <https://doi.org/10.1016/j.jma.2018.12.003> (2019).
2. Zhou, P., Gong, H. R. & Mech, J. *Behav. Biomed. Mater.* **8**, 154–164 <https://doi.org/10.1016/j.jmbbm.2011.12.001>. (2012).
3. Groh, S. Mechanical, thermal, and physical properties of Mg--Ca compounds in the framework of the modified embedded-atom method. *J. Mech. Behav. Biomed. Mater.* **42**, 88–99 (2015).
4. Daoud, S., Bouarissa, N., Benmakhlouf, A. & Allaoui, O. High-pressure effect on elastic constants and their related properties of MgCa intermetallic compound. *Phys. Status Solidi B.* **257**, 1900537. <https://doi.org/10.1002/pssb.201900537> (2020).
5. Rekab-Djabri, H. et al. Ground state parameters, electronic properties and elastic constants of CaMg3: DFT study. *J. Magnes. Alloys.* **8**, 1166–1175. <https://doi.org/10.1016/j.jma.2020.06.007> (2020).
6. Boudissa, R. et al. Mika Sillanpää. Prediction study of structural, electronic and optical properties of 4C16H10Br2O2 Bis (m-bromobenzoyl) methane crystals. *Biochem. Biophys. Rep.* **37**, 101601. <https://doi.org/10.1016/j.bbrep.2023.101601> (2024).
7. Ceperley, D. M. & Alder, B. Ground state of the electron gas by a stochastic method. *Phys. Rev. Lett.* **45** (7), 566. <https://doi.org/10.1103/PhysRevLett.45.566> (1980).
8. Perdew, J. P. & Zunger, A. Self-interaction correction to density-functional approximations for many-electron systems. *Phys. Rev. B.* **23** (10), 5048–5079. <https://doi.org/10.1103/PhysRevB.23.5048> (1981).
9. Vanderbilt, D. Soft self-consistent pseudopotentials in a generalized eigenvalue formalism. *Phys. Rev. B.* **41**, 7892–7895. <https://doi.org/10.1103/PhysRevB.41.7892> (1990).
10. Monkhorst, H. J. & Pack, J. D. Special points for Brillouin-zone integrations. *Phys. Rev. B.* **13**, 5188–5192. <https://doi.org/10.1103/PhysRevB.13.5188> (1976).
11. Otero-de-la-Roza, A. & Luanía, V. Gibbs2: A new version of the quasiharmonic model code. II. Models for solid-state thermodynamics, features and implementation. *Comput. Phys. Commun.* **182**, 2232–2248. <https://doi.org/10.1016/j.cpc.2011.05.009> (2011).
12. Daoud, S., Bouarissa, N. & Bioud, N. P. K. Saini. High-temperature and high-pressure thermophysical properties of alp semiconducting material: A systematic Ab initio study. *Chem. Phys.* **525**, 110399. <https://doi.org/10.1016/j.chemphys.2019.110399>
13. Amari, S. & Daoud, S. *Comput. Condens. Matter* **33**, e00764. [https://doi.org/10.1016/0022-3697\(95\)00265-0](https://doi.org/10.1016/0022-3697(95)00265-0) (2022).
14. Birch, F. Finite elastic strain of cubic crystals. *Phys. Rev.* **71**, 809–824. <https://doi.org/10.1103/PhysRev.71.809> (1947).

15. Benguesmia, F., Benamrani, A., Boutahar, L., Rekab-Djabri, H. & Daoud, S. Hydrostatic pressure effect on the structural parameters of GaSb semiconducting material: Ab-initio calculations. *J. Phys. Chem. Res.* **1** (2), 25–30. <https://doi.org/10.58452/jpcr.v1i2.24> (2022).
16. Daoud, S., Saini, P. K. & Rekab-Djabri, H. Theoretical Prediction of Some Physical Properties of  $BxAl_{1-x}Sb$  Ternary Alloys. *J. Nano-Electron. Phys.* **12**, 06008. [https://doi.org/10.21272/jnep.12\(6\).06008](https://doi.org/10.21272/jnep.12(6).06008) (2020).
17. Ghebouli, B. et al. Structural, elastic and electronic properties for  $M_2XC$  ( $M=$  Ti and Cr,  $X=$  Ga and Al) phases from Ab initio calculations. *Acta Metall. Sin.* **24** (4), 255–270. <https://doi.org/10.11890/1006-7191-114-255> (2011).
18. Belkhir, M. L., Gueddouh, A., Faid, F. & Rougab, M. The structural, electronic, magnetic, mechanical, and lattice dynamical properties of the novel full-heusler alloys  $Mn_2HfX$  ( $X=$  Si and Ge): Ab initio study. *J. Superconduct. Nov. Magnet.* **36**, 131. <https://doi.org/10.1007/s10948-022-06431-1> (2023).
19. Kong, F. & Jiang, G. Phase transition, elastic, thermodynamic properties of zinc-blende bese from first-principles. *Phys. B* **404**, 3935–3940. <https://doi.org/10.1016/j.physb.2009.07.131> (2009).
20. Boufadi, F. et al. First principles study of mechanical stability and thermodynamic properties of  $K_2S$  under pressure and temperature effect. *Acta Phys. Pol. A* **129**, 315–322. <https://doi.org/10.12693/APhysPolA.129.315> (2016).
21. Daoud, S. Structural phase transition, electronic and elastic properties in  $TI_3X$  ( $X=$  N, P, As) compounds: Pressure-induced effects. *Comput. Mater. Sci.* **111**, 532–533. <https://doi.org/10.1016/j.commatsci.2015.09.022> (2016).
22. Firdous, F., Ain, Q., Issa, S. A. M., Zakaly, H. M. H. & Munir, J. A spin-polarized analysis of the half-metallicity, mechanical, structural and optoelectronic attributes of full-Heusler  $XVC_2$  ( $X=$  B and P) alloys. *RSC Adv.* **14**, 34679. <https://doi.org/10.1039/d4ra06555g> (2024).
23. Benmakhlof, A., Benmakhlof, A., Allaoui, O. & Daoud, S. Theoretical study of elastic and thermodynamic properties of cusc intermetallic compound under high pressure. *Chin. J. Phys.* **57**, 179–188. <https://doi.org/10.1016/j.cjph.2018.11.017> (2019).
24. Zhao, Y. N. et al. Ab initio calculations of structural, lattice dynamical, and thermodynamic properties of Zinc-Blende hgse and CdSe. *Adv. Condens. Matter Phys.* <https://doi.org/10.1155/2024/5538895> (2024).
25. Hao, Y.-J., Cheng, Y., Wang, Y.-J. & Chen, X.-R. *Chin. Phys.* **16** 217. <http://iopscience.iop.org/1009-1963/16/1/037> (2007).
26. El Krimi, Y., Masrour, R. & Jabar, A. Electronic, magnetic, elastic, thermal and thermoelectric proprieties of  $Co_2MnZ$  ( $Z=$  al, Ge, Sn). *J. Mol. Graph. Model.* **114**, 108165. <https://doi.org/10.1016/j.jmgm.2022.108165> (2022).
27. Zhang, X. D., Ying, C. H., Quan, S. Y. & Li, Z. J. Ab initio study of the structural, phonon, elastic and thermodynamic properties of the ordered  $Ge_0.5Sn_0.5$  cubic alloy under high pressure. *Comput. Mater. Sci.* **58**, 12–16. <https://doi.org/10.1016/j.commatsci.2012.02.004> (2012).
28. Bioud, N. & Benchiheub, N. Pressure effect on some physical properties of calcium oxide materia. *Chem. Phys. Impact.* **7**, 100342. <https://doi.org/10.1016/j.chphi.2023.100342> (2023).
29. Bioud, N. & Benchiheub, N. Mechanical and thermal behavior of semiconducting cadmium oxide at High-Pressure. *Ann. West Univ. Timisoara-Phys.* **66**, 142–156 <https://doi.org/10.2478/awutp-2024-0009> (2024).
30. Benkara-Mohammed, N., Bioud, N. & Benchiheub, N. Hydrostatic pressure response of semiconducting GaSb applying a semi-empirical approach. *Comput. Condens. Matter.* **39** (2), e00895. <https://doi.org/10.1016/j.cocom.2024.e00895> (2024).
31. Bioud, N., Sun, X. W., Daoud, S., Song, T. & Liu, Z. J. Structural stability and thermodynamic properties of  $BSb$  under high pressure and temperature. *Mater. Res. Express.* **5**, 085904. <https://doi.org/10.1088/2053-1591/aad3a5> (2018).
32. Ghebouli, B., Ghebouli, M. A. & Fatmi, M. A. Structural, elastic, electronic, optical and thermal properties of cubic perovskite  $CsCdF_3$  under pressure effect. *Eur. Phys. J. Appl. Phys.* **53**, 30101. <https://doi.org/10.1051/epjap/2010100318> (2011).
33. Sultan, N. M., Badri Albarody, T. M., Mohsin Al-Jothery, H. K., Abdullah, M-A. & Mohammed, H. G. Obodo. Thermal expansion of 3 C-SiC obtained from in-situ X-ray diffraction at high temperature and first-principal calculations. *Materials* **15** (18), 6229. <https://doi.org/10.3390/ma15186229> (2022).
34. Behera, D. et al. A comprehensive first-principles investigation of  $SnTiO_3$  perovskite for optoelectronic and thermoelectric applications. *Crystals* **13** (3), 408. <https://doi.org/10.3390/cryst13030408> (2023).
35. Daoud, S., Bioud, N. & Saini, P. K. Finite temperature thermophysical properties of  $MgCu$  intermetallic compound from quasi-harmonic Debye model. *J. Magnes. Alloys* **7**, 335–344 <https://doi.org/10.1016/j.jma.2019.01.006> (2019).
36. Tian, W. & Chen, H. Theoretical investigation of the mechanical and thermodynamics properties of  $Nb_3Ga$  superconductor under pressure. *J. Alloy Comp.* **648**, 229–236. <https://doi.org/10.1016/j.jallcom.2015.06.202> (2015).
37. Duffy, T. S. & Wang, Y. *Rev. Mineral.* **37** (1999).

## Acknowledgements

This work was funded by the Researchers Supporting Project Number (RSP2025R265), King Saud University, Riyadh, Saudi Arabia.

## Author contributions

Conceptualization: A. Benmakhlof, N. Bioud, Mika SillanpääMethodology: M.A. Ghebouli, Razan A. Alshgari, Saikh Mohammad, Validation: M. Fatmi.

## Declarations

### Competing interests

The authors declare no competing interests.

### Additional information

Correspondence and requests for materials should be addressed to M.F.

Reprints and permissions information is available at [www.nature.com/reprints](http://www.nature.com/reprints).

**Publisher's note** Springer Nature remains neutral with regard to jurisdictional claims in published maps and institutional affiliations.

**Open Access** This article is licensed under a Creative Commons Attribution-NonCommercial-NoDerivatives 4.0 International License, which permits any non-commercial use, sharing, distribution and reproduction in any medium or format, as long as you give appropriate credit to the original author(s) and the source, provide a link to the Creative Commons licence, and indicate if you modified the licensed material. You do not have permission under this licence to share adapted material derived from this article or parts of it. The images or other third party material in this article are included in the article's Creative Commons licence, unless indicated otherwise in a credit line to the material. If material is not included in the article's Creative Commons licence and your intended use is not permitted by statutory regulation or exceeds the permitted use, you will need to obtain permission directly from the copyright holder. To view a copy of this licence, visit <http://creativecommons.org/licenses/by-nc-nd/4.0/>.

© The Author(s) 2025